

Modelling of thermal behaviour of a direct solar drier possessing a chimney: Application to the drying of cassava

K.B. Koua^{1*}, P. Gbaha², E.P.M. Koffi², W.F. Fassinou¹ and S. Toure¹

¹Laboratoire d'Energie Solaire, Université de Cocody- Abidjan, 22 BP 582 Abidjan 22 (Cote D'Ivoire)

²Laboratoire d'Energie Nouvelle et Renouvelable, Institut National Polytechnique, Félix Houphouët- Boigny de Yamoussoukro (Cote D'Ivoire).
kouakb@yahoo.fr*

Abstract

The aim of this work is to study a direct solar drier possessing a chimney for agricultural products. The establishment of heat and mass balances leads to a system of two differential equations translating the thermal behaviour of the solar chimney. This system is completed with another differential equation giving the evolution of the product temperature according to the time. Then, the mathematical model is validated by comparing the theoretical results with the experimental ones. Cassava has been chosen as the product to be dried because of its various uses in the food. The results showed that the drying of the product is affected by the drying air temperature and the product characteristics.

Keywords: Drying kinetic, Mathematical model, Moisture Content, Cassava, Solar.

Introduction

Solar drying is an age old practice. In African villages foods are spread on the ground and exposed under the sun to get dried. However, this method has many disadvantages. It depends largely on the climatic conditions and requires a long time of exposure to sun light, in particular, to ultraviolet rays. This leads to the deterioration of the dried products. Besides, this method does not permit the drying of large quantities of products. To improve this method of natural drying under the sun, scientific works were initiated which started in 1920s first by Lewis (1921) and then Sherwood (1929a, 1929b, 1931) who proposed an equation of diffusion to describe the drying. The setting in evidence by Philip and Vries (1957) especially the role operated by the heat transfer on the mass transfer has been an important contribution. Since then the theories, already established, permit the scientific and technological developments that facilitate drying of industrial quantities by day and preserved organoleptic characteristics (odour, flavour, texture and colour) and nutritional quality. Tiris and Dincer (1996) have proposed a small solar drier and have made an experimental comparison between natural sun drying and the artificial one. For this drier, the air is heated using an electrical heater, then a solar collector. They established that the artificial drying is more successful than natural sun drying. They then showed that the artificial drying reduces the drying time significantly and provides a better product quality. Akpinar *et al.* (2003) proposed a convective drier for red pepper. It consisted of a fan, heaters and drying chamber. The airflow rate was adjusted by the fan speed control. The heating system consisted of an electric 3000 W heater placed inside the duct. Smitabhindu *et al.* (2008) demonstrated the potentiality of solar-assisted convection drier for production of quality dried fruits. This drying system has a capacity of drying 250 kg of products with an auxiliary heat source using an LPG gas burner.

Although the drying is a highly developed technique, it gives rise to very high energy consumption (Caputo *et al.*, 2003). In order to reduce it, it is necessary to select an efficient drying system. It is for this reason that in the past years the interest in using solar driers has increased. Solar energy is preferred to other sources of energy because of it is abundant, inexhaustible and non-polluting. It can be tapped at relatively low cost and has no associated environmental dangers.

Thus, the study of the solar drying behaviour has been of great interest for several researchers. Youcef-Ali *et al.* (2001) have studied a solar batch drier based on the equation of the heat applied to the product and on the equation of the drying rate. Koyuncu (2006) tested the behaviour of various designs of flat plate low temperature air-heating solar collectors for crop drying applications. Kumar and Tiwari (2006) reported thermal modelling of jiggery drying in a natural convection solar greenhouse drier. Barnwal and Tiwari (2008) reported solar drying of grape using hybrid photovoltaic thermal greenhouse dryer and developed a multilinear expression to predict moisture evaporation during drying. Mohanraj and Chandrasekar (2008) fabricated and tested an indirect forced convection solar drier integrated with sensible heat storage material for copra drying.

In the present study, a direct new type natural convection solar drier consisting of a chimney coupled to a drying chamber is designed, constructed and investigate experimentally. Experiments for drying of cassava were performed. The modelling and thermal performance results of the solar drier have been presented. In addition, the drying kinetic of cassava was studied.

Theoretical study of the solar drier

The mathematical modelling consists to simulate the phenomena of heat and mass transfer by a set of equations putting in evidence the energetic state of the different parts of the direct solar drier (chimney and drying

chamber). A schema of the direct solar drier using a chimney is given by the Fig.1 which illustrates its different parts (Gbaha *et al.*, 2007; Koua, 2007).

Fig.1. A schema of the direct solar drier using a chimney

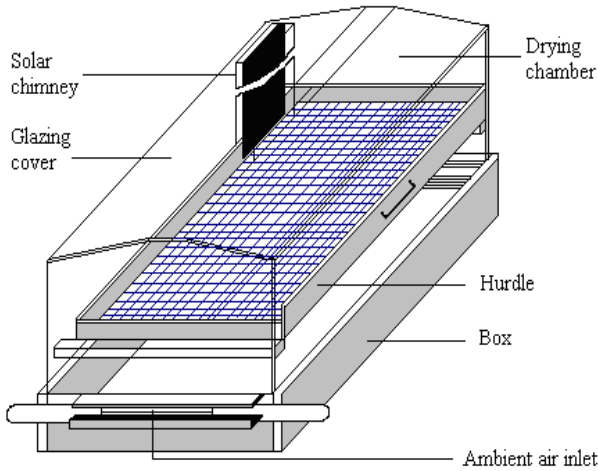
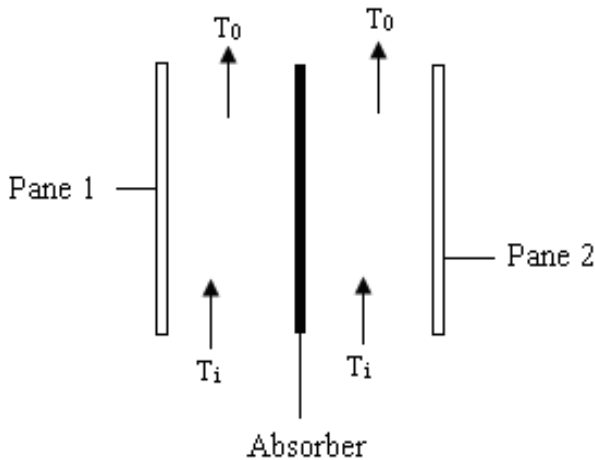


Fig.2. Diagram of the solar chimney



To simplify the study of heat and mass transfers, the following hypotheses are supposed:

- The various properties thermo physical remain constants;
- The cover in glass and the absorber have uniform temperatures;
- The temperature and the moisture content are supposed uniforms inside the product.

Solar chimney

The solar chimney comprises a steel plate which has 0.1 m^2 area and painted in mat black. It is a vertical plane collector that assures the aerodynamic working of the drier (Fig.2). It behaves like a thermosiphon in a natural convection. The absorber receives the solar flux. A part of this energy is stored and the other part is exchanged by convection with the fluid (air) and by convection and radiation with the glass cover. The balances of energy

exchange for the absorber and the glass cover of the chimney are written as follows:

For the absorber:

$$M_c C p_c \left(\frac{dT_c}{dt} \right) = 2(\alpha\tau) A_c G_i - h_{rcv1} A_c (T_c - T_{v1}) - h_{rcv2} A_c (T_c - T_{v2}) - 2h_{ccf} A_c (T_c - T_f) \quad (1)$$

The two panes having the same temperature practically ($T_{v1} = T_{v2} = T_v$) and we will notice that $h_{rcv1} = h_{rcv2} = h_{rcv}$. The Eq. (1) becomes:

$$\frac{M_c C p_c}{2} \left(\frac{dT_c}{dt} \right) = (\alpha\tau) A_c G_i - h_{rcv} A_c (T_c - T_v) - h_{ccf} A_c (T_c - T_f) \quad (2)$$

For each cover in glass:

$$M_v C p_v \left(\frac{dT_v}{dt} \right) = \alpha_v S_v G_i + h_{rcv} S_v (T_c - T_v) - h_{cvf} S_v (T_v - T_f) - h_{rvsk} S_v (T_v - T_{sk}) - h_{cva} S_v (T_v - T_a) \quad (3)$$

Where

$$T_f = \frac{T_o + T_i}{2}$$

The coefficient of heat transfer by radiation between the cover in glass and the vault of heaven is given by Kouhila *et al.* (2001):

$$h_{rvsk} = \epsilon_v \sigma (T_{sk} + T_v) (T_{sk}^2 + T_v^2) \quad (4)$$

where σ is the constant of Stefan - Boltzmann,

T_{sk} is the temperature of the vault of heaven and is given by Swinbank relation (Swinbank, 1963):

$$T_{sk} = 0.0552 T_a^{1.5} \quad (5)$$

The coefficient of heat transfer by radiation between the absorber and the cover in glass, h_{rcv} , is given as (Duffie & Beckman, 1991):

$$h_{rcv} = \frac{\sigma (T_c^2 + T_v^2) (T_c + T_v)}{\left(\frac{1}{\epsilon_c} + \frac{1}{\epsilon_v} - 1 \right)} \quad (6)$$

The coefficients of heat transfer by convection, h_{ccf} and h_{cvf} , are calculated while using Nusselt number relation:

$$hc = \frac{Nu \lambda}{D} \quad (7)$$

Where the Nusselt number Nu is expressed by Churchill and Chu's correlation (Knudson & Rempe, 2002):

$$Nu = \left[0.825 + \frac{0.387 Ra^{\frac{1}{6}}}{\left\{ 1 + (0.492/Pr)^{\frac{9}{16}} \right\}^{\frac{8}{27}}} \right]^2 \quad (8)$$

The Rayleigh number Ra is expressed by the following relation:

$$Ra = \frac{g\beta D^3 \Delta T}{\nu} \quad (9)$$

The coefficient of heat transfer by convection between the pane and the environment, h_{cva} , is given by the relation of Mac Adams (1954):

$$h_{cva} = 5.67 + 3.86v \quad (10)$$

Some parameters characterize the thermal performance of a solar collector. These parameters are related to the collector's thermal output. The thermal output is defined as the ratio of the useful energy on the incident solar radiation, for one period. This useful energy is particularly related to the thermal losses of the system and its environment, resulting from the conductive, convective and irradiative exchanges. The thermal output for one period t_0 is determined by Karim and Hawlader (2004):

$$\eta = \frac{\dot{m} C_p \int_0^{t_0} (T_0 - T_i) dt}{A_c \int_0^{t_0} G_t dt} \quad (11)$$

In the steady state, a solar collector thermal performance is expressed by Hottel - Whillier and Bliss equation (Duffie & Beckman, 1980):

$$\eta = \frac{q_u}{A_c G_t} = F_R (\tau\alpha) - \frac{F_R U_L}{G_t} (T_i - T_a) \quad (12)$$

The coefficient F_R is the conductance factor of the absorber and is given by the classic formula of Hottel - Whillier and Bliss (Duffie & Beckman, 1991):

$$F_R = \frac{\dot{m} C_p}{A_c U_L} \left[1 - \exp\left(-\frac{F' A_c U_L}{\dot{m} C_p}\right) \right] \quad (13)$$

The factor F' is the absorber's efficiency.

The useful heat gain of a solar collector can be expressed by the following thermal performance equation given by Hottel and Whillier (1958):

$$q_u = \dot{m} C_p (T_0 - T_i) = A_c [(\tau\alpha)G_t - U_L(T_c - T_a)] \quad (14)$$

This useful heat gain can also be expressed by Hottel - Whillier and Bliss model (Duffie & Beckman, 1991):

$$q_u = A_c F_R [(\tau\alpha)G_t - U_L(T_i - T_a)] \quad (15)$$

Therefore

$$T_0 - T_i = \frac{A_c F_R}{\dot{m} C_p} [(\tau\alpha)G_t - U_L(T_i - T_a)] \quad (16)$$

According to the relation (12), the instantaneous thermal output decreases linearly when the variation of air temperature ($T_i - T_a$) increases. It is maximum and

equal to $F_R (\tau\alpha)$ when $T_i = T_a$. In the usual collector η is between 60 % and 80%. It is null when $G_t = G_{tmin}$. For $G_t < G_{tmin}$, the output is negative and the solar collector heats the atmosphere. In this case, it is necessary to stop the air circulation and the output becomes worthless.

G_{tmin} is the threshold level of incident solar flux and is defined as:

$$U_L = \frac{G_{tmin} (\tau\alpha)}{T_i - T_a} \quad (17)$$

The relation giving the difference of temperature between inlet and outlet of the solar chimney becomes:

$$T_0 - T_i = \frac{A_c F_R (\tau\alpha)}{\dot{m} C_p} (G_t - G_{tmin}) \quad (18)$$

Drying chamber

The circulation of dry air within the drying chamber leads to an exchange between this air and the product. The product receives the heat. A part is stored by the product and the other part serves to evaporate its water. The heat and mass balances allow the establishment of the following equation (Kouhila *et al.*, 2001):

$$M_p C_{pp} \left(\frac{dT_p}{dt}\right) = h_{cfp} S_p (T_f - T_p) - P_{ev} \quad (19)$$

The coefficient of heat transfer between the product and the drying air is given as:

$$h_{cfp} = \frac{Nu \lambda}{D_p} \quad (20)$$

D_p is the average diameter of the product.

The Nusselt number (Nu) and the Reynolds number (Re) are given by Kouhila *et al.* (2001):

$$Nu = 0.37 Re^{0.6} \quad (21)$$

$$Re = \frac{\rho_a v_a D_p}{\mu} \quad (22)$$

v_a is the velocity of air to the level of the product in m/s

P_{ev} is the evaporative power and is given by Kouhila *et al.* (2001) the following relation:

$$P_{ev} = M_{ps} L_v \frac{dX}{dt} \quad (23)$$

M_{ps} is the dry product mass (kg).

L_v is the latent heat of water vaporization in J/kg and is given:

$$L_v = 4186.8 (597 - 0.56 T_p) \quad (24)$$

The exchange surface of the product, noted S_p , is given by the following relation:

$$S_p = n\pi \frac{D_p^2}{4} \quad (25)$$

n is the number of dried products put on hurdle.

Resolution method

The two sets of equations can be resolved numerically using finite difference technique and by

developing MATLAB programs. The first set concerning the chimney and the second for the drying chamber. The numerical calculations have been made for a sky without major cloudy passage. Fit quality was evaluated by calculating the mean relative percentage deviation modulus, E%, according to Eq. (26). E% is an absolute value that correlates the estimated and experimental data. Low mean relative deviation modulus values (E% < 10%) indicates good fit (Rosa *et al.*, 2010).

$$E\% = \frac{100}{N} \sum_{i=1}^N \frac{|T_{\text{exp},i} - T_{\text{est},i}|}{T_{\text{exp},i}} \quad (26)$$

Where N is the number of observations, $T_{\text{exp},i}$ and $T_{\text{est},i}$ are the experimental and estimated values of the temperature.

Drying kinetics

The evolution in water loss of the product is described by a function, called the mass flux which defines the mass loss of water per unit of exchange surface and unit of time. It is noted F_m and is given by the following relation (Dissa *et al.*, 2010):

$$F_m = - \frac{M_{ps}}{S_p} \frac{dX}{dt} \quad (27)$$

This mass flux is function of the product and of the drying conditions.

This model permits to identify three distinct phases of the drying kinetics. These three phases are preceded by a preheating phase which will not be discussed here. These behaviours of the product during the drying meet again in the curve of volume retreat but also in the curve of the drying rate. Indeed, each phase is bounded by intervals of moisture content. Noting by X, the moisture content of the product, the mathematical modelling can be formulated as follows:

- Constant drying rate phase: $X > X_{cr1}$

Where X_{cr1} is the critical moisture content.

The mass flux F_m , exchanged between air drying and the product, is constant (Koua, 2007):

$$F_m = F_{\text{const}} = \frac{h_c}{L_v} (T_i - T_p) \quad (28)$$

where F_{const} is the mass flux value at constant drying rate phase.

- falling drying rate phase: $X < X_{cr1}$

This drying phase is divided into two parts.

- first falling drying rate phase: $X_{cr2} < X < X_{cr1}$

X_{cr2} delimits the zone of fast decrease of the drying rate.

The decrease of the product volume affects the exchange surface of air-product. Therefore, the mass flux decreases following a power b of the product volume which relation is given by Rakotondramirana *et al.* (2005):

$$F_m = F_{\text{const}} \left(\frac{V}{V_o} \right)^b \quad (29)$$

where b is a coefficient taking the zero value in isenthalpic phase and a value different to zero in decrease phase. Its value depends on the mass flux curve as a function of the moisture content.

- second falling drying rate phase: $X < X_{cr2}$

In this second zone of falling drying rate, the final volume of product is reached. The mass flux is expressed as follows (Rakotondramirana *et al.*, 2005):

$$F_m = F_{\text{const}} \left(\frac{V_{X_{cr2}}}{V_o} \right)^b \left(\frac{X}{X_{cr2}} \right)^a \quad (30)$$

where "a" is a critical parameter of correction depending on the drying conditions.

Experimental procedure

The works are performed in Yamoussoukro, the political capital city of Côte d'Ivoire, a West African country, located at 6.58° N latitude. The amounts of solar radiation are measured with a pyranometer Kipp and Zonen CM 10. This apparatus consists of one thermopile and a numerical integrator allowing the reading of instantaneous fluxes by digital display. It is placed in a horizontal position in order to cover the whole of the sky. The thermopile is protected from the wind and the poor meteorological conditions by two transparent hemispherical glass cups. The relative error measurement is about $\pm 2\%$.

Temperature measurements and recording at different points in the solar drier are made by chromel-Alumel thermocouples (0.001 m diameter) connected to a data acquisition chart and a computer which $\pm 0.5\text{ }^\circ\text{C}$ accuracy. The temperatures are recorded at 7 points of the system: the chimney's inlet and outlet air temperatures, the temperature of the absorber, the air temperature of the drying chamber, the glass cover temperature, the ambient temperature and the product surface temperature. The different measurements recorded are realized every 10 minutes.

A digital weighing apparatus (type Metter PL 1200 of $\pm 0.01\text{ g}$ accuracy) measures the mass loss of the product during the drying process. During each drying experiment, the weight of the products on the hurdle was measured by removing it from the drying chamber for approximately 20-30 s. These measures were undertaken every 10 min at the beginning of the experiment and 30 min at the end. Each drying kinetic experiment was carried out at least twice to check the reproducibility of the drying curves. At the end of each experiment, the dry mass of the product was estimated by drying duplicate samples in the oven-drier at 70 °C for 24 h according to the European norm EN 12145. From mass loss data and dry mass, the moisture content at each instant of drying and the drying rate of the product were determined according to the formulas:

$$X = \frac{M(t) - M_{ps}}{M_{ps}} \quad (31)$$

$$DR = \left(-\frac{dX}{dt}\right) = -\frac{1}{M_{ps}} \frac{dM}{dt} \quad (32)$$

Where X is the moisture content of product in dry basis, DR is the drying rate of product, M (t) is the mass of product at instant t and M_{ps} is the dry mass of product. Fresh cassava was used in the experiments. Before drying, the cassava was peeled and cut into slices of 30 x 15 x 40 mm (width x thickness x length) with a mechanical cutter.

The shrinkage curve of cassava was established by measuring the length, the width and the thickness of three (3) samples during drying. Measurements were carried out using a micrometer of ± 0.05 mm accuracy. These measurements were done simultaneously with the mass measurements. The dried samples obtained had the same shape as fresh samples. Assuming that the dried samples kept exactly their initial parallelepiped shape, volume of the samples at each instant t of drying was evaluated by the following expression:

$$V = \text{width} \times \text{thickness} \times \text{length} \quad (33)$$

Where V is the volume of the sample.

Results and discussion

Intensity of the solar radiation

The Fig. 3 illustrates the evolution of direct, diffuse and global components of the solar radiation for May 18, (2007). The direct luminous intensity increases progressively up to reach its maximal value of 901 W/m² at 13:00 a.m. (local hour), then fall up to reach a value of 27.2 W/m² at 18:00 p.m. (local hour). The diffuse radiation is distributed regularly around the average value of 95 W/m², that is to say 15% of the total solar radiation. Being the result of the sum of diffuse and direct radiations, the distribution of the global radiation reach a maximal value of 1060 W/m² for this sunshine.

The Fig. 4 presents the evolution of the difference of air temperature between inlet and outlet of the chimney according to solar flux. The straight line equation

Fig.3. Variation of the instantaneous flux according to the time May 18, 2007

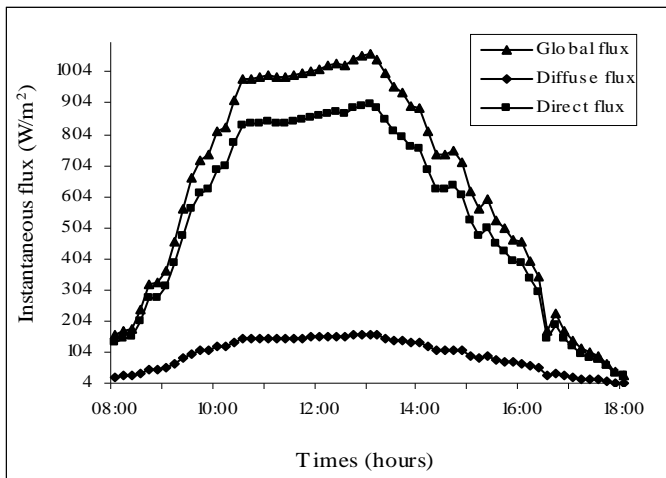
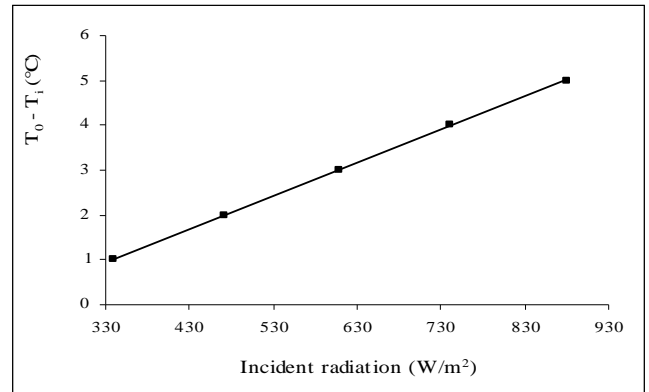


Fig.4. Variation of the difference of air temperature $T_0 - T_i$ according to the incident radiation



obtained (with $r^2 = 0.9999$) is given in the Table 1. The comparison between the equation (16) and the straight line equation of the Fig. 4 allows determining the threshold level of incident solar flux, equal in 203.62 W/m² (Table 1).

Fig.5. Variation of the chimney thermal efficiency according

$$\text{to } \frac{T_i - T_a}{G_t}$$

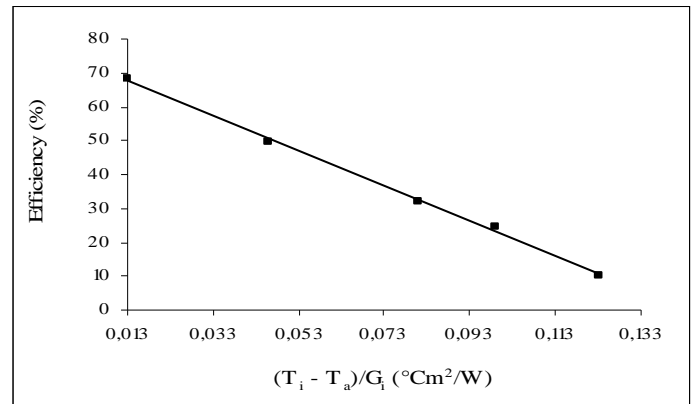


Fig.6. Variation of the absorber's temperature according to the time

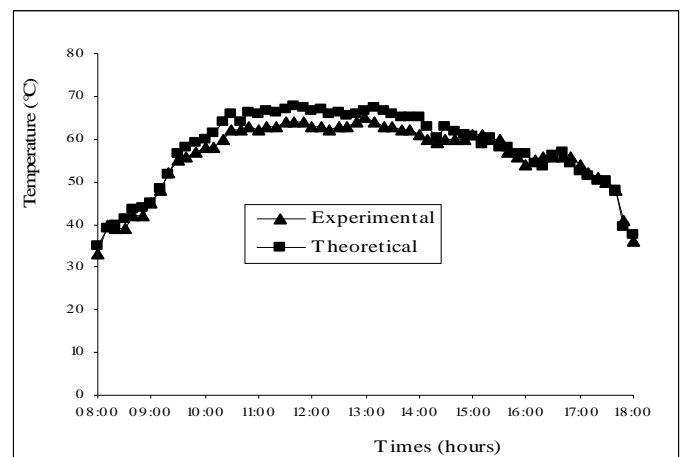


Fig.7. Variation of the temperature of the pane re-covering the absorber according to the time

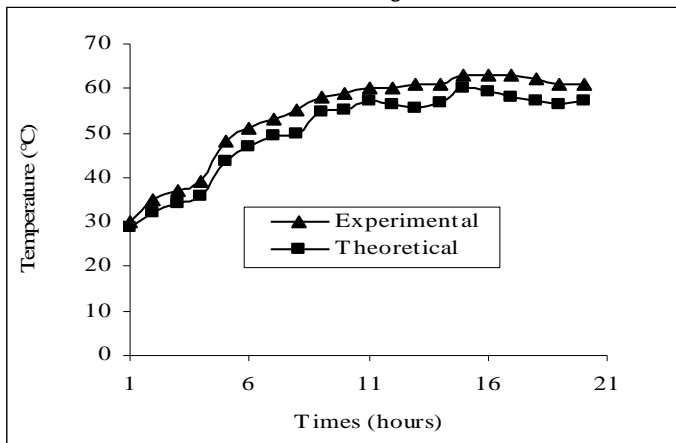


Fig.10. Variation of the cassava drying rate according to the time

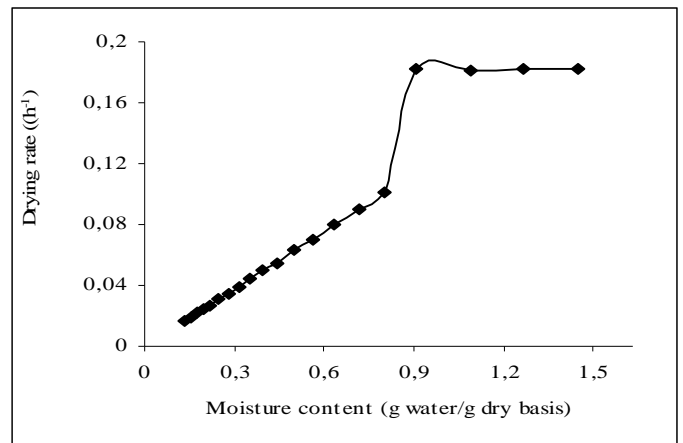


Fig.8. Variation of the cassava temperature during the drying

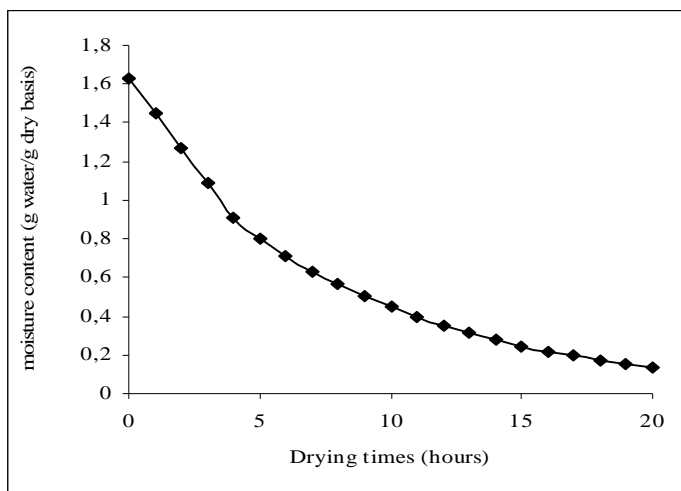


Fig.11. Variation of the cassava drying rate according to its moisture content

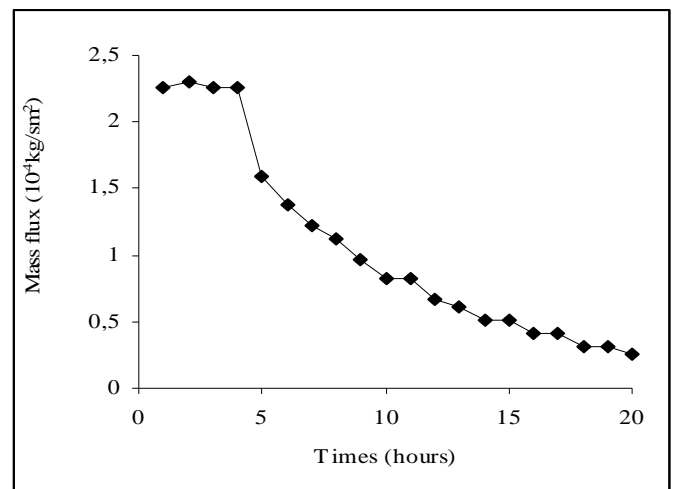


Fig.9. Variation of the moisture content of cassava with drying time

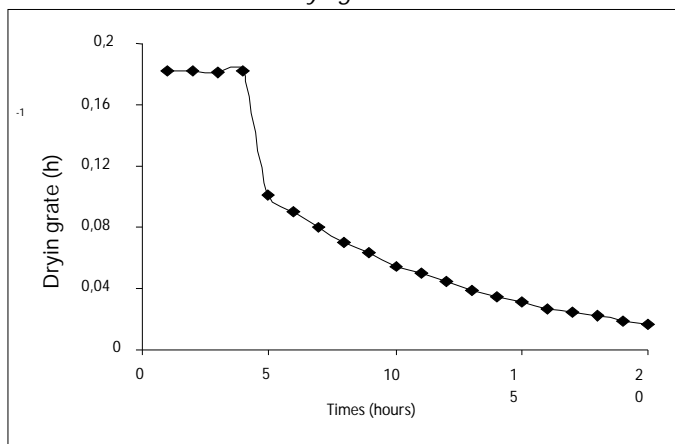


Fig.12. Variation of the mass flux of cassava according to the time

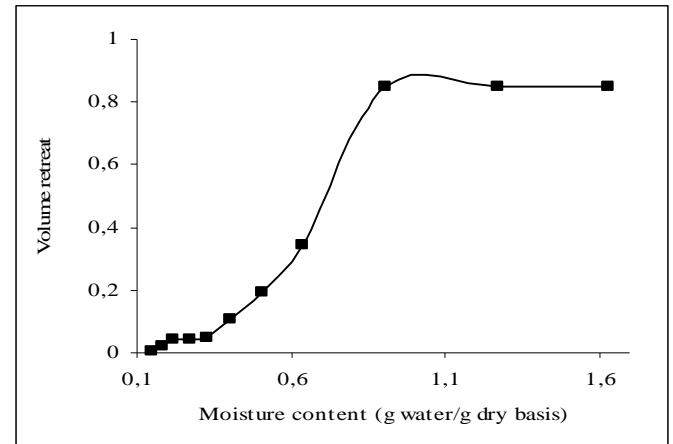


Fig.13. Variation of the cassava volume retreat according to its moisture content

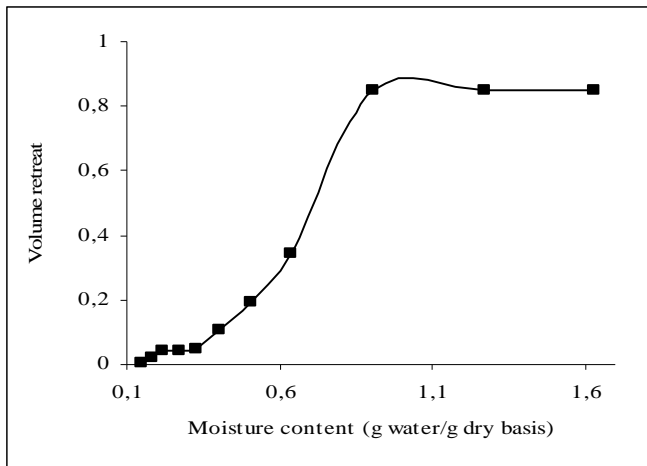


Fig.16. Variation of the moisture content of cassava according to the time for different initial masses

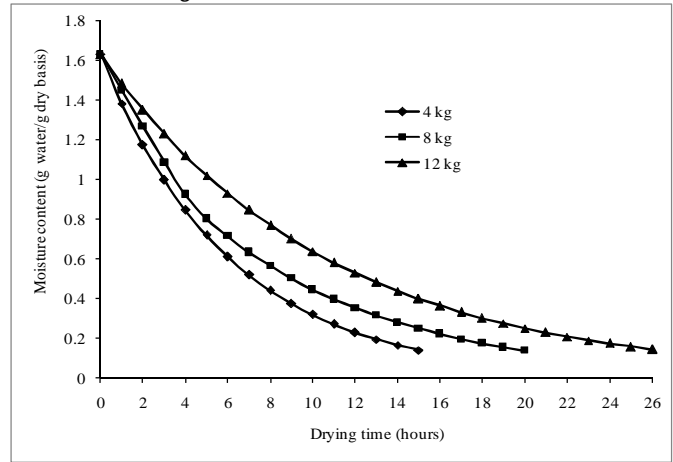


Fig.14. Variation of the temperature of cassava and the one of air drying according to the time

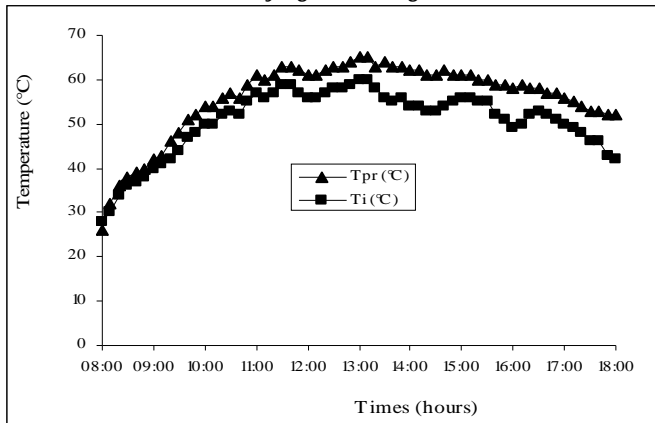


Fig.17. Variation of the moisture content of cassava according to the time for different product diameters

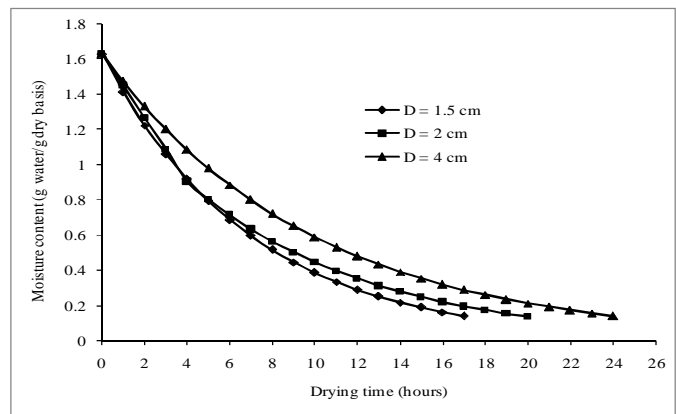


Fig.15. Variation of the moisture content of cassava according to the time for different initial moisture contents

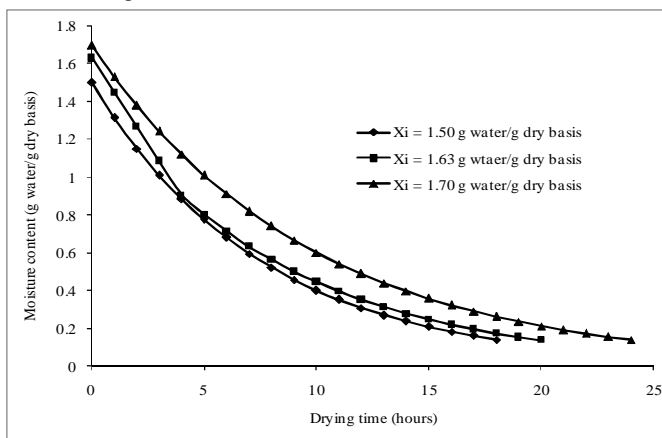


Fig.18. Variation of the global resistance to diffusion of cassava according to the product diameter

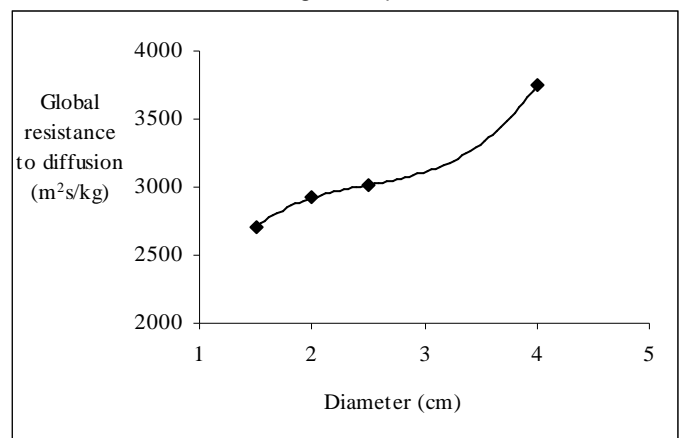


Table 1. Equation for temperature and chimney characteristic parameters

Air mass flux (kg/sm ²)	Equation for temperature	$\frac{A_c F_R (\tau\alpha)}{m C_p}$	$\frac{A_c F_R (\tau\alpha) G_{tmin}}{m C_p}$	G _{tmin} (W/m ² K)
0.1	T ₀ - T _i = 0.0074G _i - 1.5068	0.0074	1.5068	203.62

$$F_m = F_{const} \left(\frac{V}{V_o}\right)^{2.29} \quad (34)$$

- Second falling drying rate phase:

$$F_m = F_{const} \left(\frac{V_{X_{cr2}}}{V_o}\right)^{2.29} \left(\frac{X}{X_{cr2}}\right)^{1.10} \quad (35)$$

Evolution of the volume retreat with the moisture content

The mechanical characteristics of the product evolve with the moisture content. The product undergoes a distortion. One will can discern a volume retreat β_v given as:

$$\beta_v = \frac{V - V_s}{V_s} \quad (36)$$

On Fig. 13 we can observe that the product volume remains non constant during the drying and depends on its moisture content. We can also notice that two particular values of moisture content X_{cr1} and X_{cr2} subdivide the volumetric shrinkage curve in three distinct zones. Thus, above the biggest value X_{cr1} of the critical moisture contents, the volume of the product remains practically constant. Between the values X_{cr1} and X_{cr2}, the product volume decreases almost linearly with the moisture content. Below X_{cr2}, the product volume reaches a constant final value. The values of X_{cr1} and X_{cr2} are given in the Table 3. These results are appreciably equal to those given by Touré and Kibangu-Nkembo (2004) indeed they showed that the critical moisture content of cassava is 92.80 g water /100g dry basis.

the volumetric shrinkage curve in three distinct zones. Thus, above the biggest value X_{cr1} of the critical moisture contents, the volume of the product remains practically constant. Between the values X_{cr1} and X_{cr2}, the product volume decreases almost linearly with the moisture content. Below X_{cr2}, the product volume reaches a constant final value. The values of X_{cr1} and X_{cr2} are given in the Table 3. These results are appreciably equal to those given by Touré and Kibangu-Nkembo (2004) indeed they showed that the critical moisture content of cassava is 92.80 g water /100g dry basis.

Evolution of the product temperature with the time

The study of evolution of the product temperature (Fig.14) allows us to specify the different mechanisms that occur during the drying. We can notice that in the beginning of the drying, we have a transient phase where the temperature increases of an initial value until the humid temperature that corresponds to the ambient temperature. The result is that the product heats. After this transient phase, the product is in thermal balance with air drying. During this short period, the temperature of the product varies slowly with time. Then, the temperature of the product increases quickly in the second drying phase.

During the first phase, the temperature of cassava (T_{pr}) is superior to the temperature of the surrounding air (T_i), the average gap being of 3°C in spite of an important activity of drying to the surface of the samples. Beyond the previous phase, the gap between the temperature of the product and the one of air drying becomes accentuated, with an average gap that is worth 6.5°C.

Influence of the initial moisture content on the drying duration

It is obvious that, the more the moisture content of the product is elevated; the more the duration of drying is long. However, the duration of drying is not proportional to the water evaporated quantity. Fig.15 well illustrates this influence. The duration of drying for the three initials moisture contents 1.50 g water /g dry basis, 1.63 g water /g

The global thermal average loss coefficient is estimated using the equation (12) and the Fig. 5. Its estimated average value is given in Table 2.

Evolution of temperatures

The temperatures of the different parts of the chimney are represented successively on the Fig. 6 and 7. The temperature evolution is function of instantaneous incident heat fluxes. We notice a good agreement between the theoretical and experimental curves. The mean relative

Table 2. Output equation and chimney physical characteristics

Air mass flux (kg/sm ²)	output equation	F _R (τ α)	F _R U _L	F _R	U _L (W/m ² K)
0.1	$\eta = 0.744 - 5.173 \frac{T_i - T_a}{G_i}$	0.744	5.173	0.910	5.68

percentage deviation modulus (E %) is 6%. Fig. 8 represents the evolution of cassava temperature during the drying. The comparison between the theoretical and experimental curves of the cassava temperature reveals a good agreement with a mean relative percentage deviation modulus (E %) of 9%.

Table 3. Cassava characteristics moisture contents

Initial moisture content (g water /100g db)	First critical moisture content (g water /100g db)	Second critical moisture content (g water /100g db)	Equilibrium moisture content (kg water / kg db)
163.2	93	23	1.76x10 ⁻²

Evolution of the moisture content during the time

Fig. 9 represents the evolution of cassava moisture content with drying time. The moisture content decreases linearly during the first periods of drying. This is due to the evaporation taking place solely in surface; this evaporation resembles the one occurring to the free surface of a liquid. It continues until the capillary forces become weak enough and that the liquid phase becomes discontinuous and doesn't flow anymore. The humidity transfer in liquid phase toward the surface stops in this instant. However, one notes the apparition of an evaporation front that propagates toward the interior of product. It is the second drying phase. During this phase, one notes that the moisture content falls considerably.

The Fig.10 and 11 present the evolution of cassava drying rate respectively according to the time and its moisture content. Fig. 12 gives the evolution of the mass flux according to the time. The two curves Figs. 11 and 12 put in evidence the different phases of the drying process. On Fig.10 one can see that the phase 1 lasts 4 hours, whereas the phase 2, shorter, lasts 1 hour. The phase 3, the longest, lasts 15 hours for final moisture content X_f of 13.69 g water /100g dry basis. The multiple regression analysis and analysis of Fig.12 and 13 allow determining the accepted functions of the mass flux.

- Constant drying rate phase:

$$F_m = F_{const} = 2.25 \times 10^{-4} \text{ kg/sm}^2$$

- first falling drying rate phase:

dry basis and 1.70 g water /g dry basis, is respectively of 18 hours, 20 hours and 24 hours.

Influence of the product characteristics

The Fig.16 illustrates the influence of the product mass on its moisture content. It shows that during the drying, the moisture content of 12 kg of cassava remains more important than 4 kg. For the same product, increasing the mass implies increasing the number of samples put on hurdle of the drier. Hence, it is deduced that each sample receives less energy. Thus, the increasing of the mass increases the duration of drying. However, 26 hours are sufficient to dry 12 kg of product put on hurdle. The drying duration of 4 kg and 8 kg of cassava is respectively of 15 hours and 20 hours. Fig.17 presents the influence of the product diameter on its moisture content. The product diameter increasing leads to more resistance for diffusion. It is deduced that the increasing of the product diameter leads to a more slow decrease of the moisture content at the time of the drying. The duration of drying for the three product diameters 1.5 cm, 2 cm and 4 cm is respectively of 17 hours, 20 hours and 24 hours. This implied that the convective solar drier operated more efficiently during drying of small thickness samples of cassava slices. Fig.18 illustrates the influence of the cassava diameter D_p on the global resistance to diffusion R_{ds} . This global resistance to the diffusion is expressed by the following relation (Touré & Kibangu-Nkembo, 2004; Koua *et al.*, 2007):

$$X - X_f = C \exp\left(-\frac{A_s}{R_{ds}} t\right) \quad (37)$$

C is the constant of integration and is given by: $C = X_i - X_f$

The analysis of the Fig.18 reveals that the global resistance to diffusion R_{ds} and the cassava diameter D_p are strongly correlated. Increasing cassava diameter increases the global resistance to diffusion.

Conclusion

The theoretical and experimental study of the direct solar drier possessing a chimney allowed, first, the measure of the components of the solar radiance and the temperatures of the different parts of the drier; second, it allowed the determination of the curves of drying kinetics. As for the factors that influence the drying kinetics, we can affirm that the drying duration of the product depends on several factors such as the initial mass of the product, its initial moisture content, its diameter and the air drying temperature. A mathematical model that describes the thermal behaviour of the drier has been developed. This model allowed plotting the evolution of the temperature of the different parts of the drier. A good agreement between the theoretical and experimental results was achieved.

References

- Akpınar EK Bicer Y and Yildiz C (2003) Thin layer drying of red pepper. *J. Food Engg.* 59, 99-104.
- Barnwal P and Tiwari GN (2008) Grape drying using hybrid photovoltaic thermal (PV/T) greenhouse dryer: an experimental study. *Solar Energy.* 82,1131-1144.
- Caputo AC Scacchia F and Pelagagge PM (2003) Disposal of by-products in olive oil industry: waste-to-energy solutions. *Appl. Therm. Engg.* 23(2), 197-214.
- Dissa AO Desmorieux H Savadogo PW Segda BG and Koulidiati J (2010) Shrinkage, porosity and density behaviour during convective drying of spirulina. *J. Food Engg.* 97, 410-418.
- Duffie JA and Beckman WA (1991) Solar engineering of thermal process. *John Wiley and Sons.* NY. pp: 197-249.
- Gbaha P Yobouet Andoh H Kouassi Saraka J Kamenan Koua B and Toure S (2007) Experimental investigation of a solar dryer with natural convection heat flow. *Renew. Energy.* 32, 1817 - 1829.
- Hottel HG and Whillier A (1958) Evaluation of flat - plate collector performance. *Trans. Conf. Use of solar Energy II, Thermal Process, University of Arizona. USA.* pp: 74 - 104.
- Karim MA and Hawlader MNA (2004) Development of solar air collectors for drying applications. *Energy Convers. Manage.* 45, 329 -344.
- Knudson DL and Rempe JL (2002) In Vessel retention modeling capabilities of SCDAP/RELAP5-3D. *Proceedings of ICON10 tenth Intl. Conf. on nuclear Engg. Arlington. VA. USA.* pp: 1-9.
- Koua KB (2007) Etude expérimentale d'un séchoir solaire direct utilisant un circulateur thermique. Thèse de Doctorat de troisième cycle. Laboratoire d'Énergie Solaire. *Université de Cocody - Abidjan, Côte d'Ivoire.*
- Koua KB Fassinou WF Gbaha P and Touré S (2007) Etude expérimentale de la cinétique de séchage du manioc dans un séchoir solaire direct muni d'un circulateur thermique. *Rev. Ivoir. Sci. Technol.* 09,11-26.
- Kouhila M Belghit and Dagenet M (2001) Modélisation et expérimentation du fonctionnement d'un séchoir solaire convectif pour plantes aromatiques. *IEEE.* pp ; 181 -188.
- Koyuncu T (2006) Performance of various designs of solar air heaters for crop drying applications. *Renew. Energy.* 31, 1073-1088.
- Kumar A and Tiwari GN (2006) Thermal modelling of a natural convection greenhouse drying system for jiggery: an experimental validation. *Solar Energy.* 80,1135-1144.
- Lewis WK (1921) The rate of drying of solids materials. *Ind. Eng. Chem.* 13 (5), 427 - 432.
- Mac Adams WH (1954) Heat transmission. 3rd ed. *Mc Graw Hill, NY.*
- Mohanraj M and Chandrasekar P (2008) Comparison of drying characteristics and quality of copra obtained in a forced convection solar drier and sun drying. *J. Sc. & Ind. Res.* 67,381-385.
- Philip JR and De Vries DA (1957) Moisture movement in porous materials under temperature gradient. *Trans. Amer. Geophys. Union.* 38 (2), 222 - 232.

19. Rakotondramirana H Morau D and Adelard L (2005) Modélisation du séchage solaire : application au séchage en couche mince des boues solides des stations d'épuration. *12^{ème} Journées Internationales de thermique, Tanger. Maroc.* pp : 203 - 206.
20. Rosa GS Moraes MA and Pinto LAA (2010) Moisture sorption properties of chitosan. *LWT-Food Sci. Technol.* 43, 415-420.
21. Sherwood T K (1929) the drying of solids 1. *Int. Engg. Chem.* 21 (1), 12-16.
22. Sherwood TK (1929) the drying of solids 2. *Int. Engg. Chem.* 21 (2), 976-980.
23. Sherwood TK (1931) Application of the theoretical diffusion equations of drying of solids. *Trans. Am. Inst. Chem. Engrs.* 27, 190 - 202.
24. Smitabhindu R Janjai S and Chankong V (2008) Optimization of a solar-assisted drying system for drying bananas. *Renew. Energy.* 33, 1523-1531.
25. Swinbank WC (1963) Long wave radiation from clear skies. *QJ Roy Meteor Soc.* pp: 89.
26. Tiris C Tiris M and Dincer I (1996) Experiments on a new small-scale solar dryer. *Appl. Th. Engg.* 16 (2), 183- 187.
27. Touré S and Serge Kibangu- Nkembo (2004) Comparative study of natural solar drying of cassava, banana and mango. *Renew. Energy.* 29, 975 - 990.
28. Youcef Ali S, Messaoudi H, Desmons JY, Abene A and Leray M (2001) Determination of the average coefficient of internal moisture transfer during the drying of a thin bed of potato slices. *J. Food Engg.* 45, 95-101.

Nomenclature

A_c : surface area of chimney, m^2
 A_s : specific surface of product, m^2/kg
 a : thermal diffusivity, m^2/s
 C_p : specific heat, $J/kg K$
 D : characteristic dimension, m
 F_m : mass flux, kg/m^2s
 G_i : incident solar radiation, W/m^2
 Gr : Grashof number
 G_t : total incident solar radiation, W/m^2
 g : acceleration of gravity, m/s^2
 h_c : coefficient of heat transfer by convection, W/m^2K
 h_r : coefficient of heat transfer by radiation, W/m^2K
 L_v : latent heat of water vaporization, J/kg
 M : mass, kg
 •
 \dot{m} : air mass flux, kg/s
 Nu : Nusselt number
 P_{ev} : evaporative power, J/s
 Pr : Prandtl number
 q_u : useful heat gain, W/m^2
 Ra : Rayleigh number
 R_{ds} : overall resistance to diffusion, m^2s/kg
 Re : Reynolds number
 r : correlation coefficient
 S : surface, m^2
 t : time, s

T : temperature, $^{\circ}C$

U_L : overall heat loss coefficient, W/m^2K

V : volume, m^3

v : velocity, m/s

X : product moisture content, $g\ water/g\ dry\ basis$

Greek Symbols

α : absorber absorptivity coefficient

β : coefficient of volumetric expansion, $1/K$

β_v : volume retreat

ε : emissivity coefficient

η : thermal output

λ : conductivity coefficient, W/mK

μ : dynamic viscosity, $kg/m.s$

ν : kinematic viscosity, m^2/s

ρ_a : air volume mass, kg/m^3

σ : Stefan-Boltzmann constant, W/m^2K^4

τ : glass transmittivity coefficient

Subscripts

a : ambient

c : absorber

cr : critical

f : fluid (air)

i : inlet of chimney

o : outlet of chimney, initial

p : product

s : dry

sk : sky

The values of thermo-physical parameters used in analysis are:

- glass volume mass: $\rho_v = 2722\ kg/m^3$

- absorber volume mass : $\rho_c = 7850\ kg/m^3$

- glass specific heat : $C_{p_v} = 794\ J/kg\ K$

- absorber specific heat : $C_{p_c} = 459\ J/kg\ K$

- Stefan Boltzmann constant: $\sigma = 5.6. 10^{-8}\ W/m^2k^4$

- glass emissivity coefficient : $\varepsilon_v = 0.95$

- absorber emissivity coefficient: $\varepsilon_c = 0,95$

- glass absorptivity coefficient: $\alpha_v = 0,82$

- absorber absorptivity coefficient: $\alpha_c = 0,90$

- glass transmittivity coefficient: $\tau_v = 0,90$